Role of Lone-Pairs in Internal Rotation Barriers

Vojislava Pophristic, Lionel Goodman,* and Nikhil Guchhait

Wright and Rieman Chemistry Laboratories, Rutgers University, New Brunswick, New Jersey 08903

Received: March 21, 1997[⊗]

An in-depth understanding of internal rotation barrier formation and energetics for dimethyl ether, protonated dimethyl ether, methanol, and their sulfur analogs is provided by dissecting the barrier into Pauli exchange steric repulsion, σ-lone-pair reorganization, and π hyperconjugation. The combined natural bond orbital, symmetry, and relaxation analysis demonstrates that oxygen σ lone-pairs play an important (sometimes dominant) role in controlling barrier heights. In dimethyl ether the increased steric contact brought about by simultaneous rotation of the methyl groups causes the COC angle to widen, in turn increasing the σ lone-pair p character, which leads to large lone-pair reorganization energy. Steric repulsion contributes to the dimethyl ether >4 kcal/mol barrier energy in only a minor way even though the steric contact can be looked at as the origin of the lone-pair increased p character. Absence of a σ lone-pair in acid media predicts a drastically lowered barrier (i.e. ∼1 kcal/mol). In methanol the increase in O atom lone-pair p character and associated lone-pair reorganization energy is strongly reduced, leading to an also greatly lowered barrier. Lone-pair σ reorganization effects are smaller in the sulfur-containing compounds, and C−S (σ) bond weakening is predicted to become the dominant barrier energy controlling term.

I. Introduction

In a recent investigation[1] we considered the origin of the dimethyl ether internal rotation barrier by partitioning the barrier energy into relaxation, natural bond orbital, and symmetry terms and pointed out that the largest contribution to the simultaneous methyl rotation barrier energy is due to increased p character in the oxygen σ lone-pair on going to the barrier top (Figure 1). This analysis showed in particular that the origin of the barrier can be fully understood only by taking into account the lone-pair rehybridization as well as increased Pauli exchange repulsion between the two in-plane C−H methyl orbitals in steric contact at the barrier top. The ∼5° opening of the COC angle accompanying internal rotation occurring because of the steric repulsion is responsible for the increased p character with concomitant decreased s character.

The key to understanding the barrier is the large decrease in the rigid rotation barrier when relaxation occurs. Rigid rotation freezes the geometry at the equilibrium geometry except for the dihedral angle that describes methyl torsion. The rigid rotation barrier energy of dimethyl ether is calculated to be nearly 900 cm^{-1} higher than the fully relaxed (and accepted) 1600 cm^{-1} simultaneous methyl rotation barrier,[1−4] illustrating the high strain in the rigid rotation SS conformer. The effect of relaxation is that the steric repulsion energy strongly decreases, but concomitantly the oxygen σ lone-pair reorganization energy strongly increases (π interaction energies (which include hyperconjugation effects), found to give important but not dominant barrier energy contributions, are relatively relaxation unaffected).[1] It is the increased top-of-barrier steric contact in the frozen conformer that is the origin of the major relaxation (i.e., the opening of the COC angle), which leads to the large σ reorganization energy.

Since this result for dimethyl ether seems to be inconsistent with the π fragment[5,6] and Pauli exchange repulsion[7] models for barrier energies, it raises the question of the general role of lone-pairs in barrier energetics, calling for a closer look at barrier energetics in lone-pair molecules. Analysis of barrier energetics in five prototype molecules with varying steric and electronic interactions: dimethyl ether (DME), protonated dimethyl ether (PDME), methyl alcohol, dimethyl sulfide (DMS), and methanethiol (MT) is therefore undertaken in the present study. This investigation of methyl torsional barriers in oxygen and sulfur molecules brings out the importance of energy effects due to charge rearrangements associated with methyl internal rotation. The connection between charge distributions and potential energy surfaces is a cornerstone of modern electronic structure theory. Moreover, rotational barriers have important applications in the action of biologically relevant molecules (e.g., in the bacteriorhodopsin photocycle[8a] and in drug design[8b−d]). They play important roles in stereospecific[9a,b] and proton transfer[9c] reactions and are a factor in nucleic acid packing in DNA. Additionally, lasing action in recently developed ultraviolet laser dyes is torsionally driven.[10] We have included protonated dimethyl ether in this study because of its biological relevance

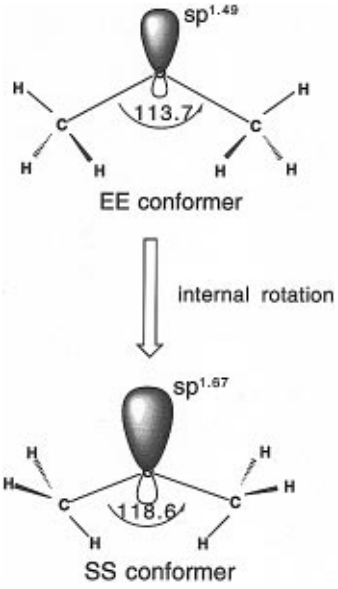

Figure 1. Schematic depiction of oxygen σ lone-pair orbital reorganization accompanying internal rotation in dimethyl ether.

[⊗] Abstract published in *Advance ACS Abstracts,* May 15, 1997.

S1089-5639(97)01020-7 CCC: $14.00

TABLE 1: Partitioning of Fully Relaxed Barrier Energy into Kinetic and Potential Energy Terms in Oxygen-Containing Compounds (cm^{-1})[a]

ΔE[b]	dimethyl ether EE→SS HF/6-31G(2d,p)	protonated dimethyl ether EE→SS HF/6-311++G	methanol E→S HF/6-31++G(d,p)
barrier	1580	260	400
virial theorem discrepancy[c]	100	60	30
ΔT	−1480	−200	−430
ΔV_{ne}	237 980	138 990	22 070
ΔV_{ee}	−111 410	−65 710	−9560

[a] Rounded to nearest 10 cm^{-1}. Positive values are barrier forming. [b] Difference between fully relaxed top-of-barrier (in-plane methyl hydrogen(s) rotated by 180°) and equilibrium conformer energy terms. ΔT = kinetic energy change, ΔV_{ne} = nuclear−electron attraction energy change, ΔV_{ee} = electron−electron repulsion energy change. [c] Fully relaxed barrier energy + ΔT.

and to provide a basis for understanding acid media effects on the internal rotation barrier of lone-pair molecules.

II. Computations

Three types of calculations were necessary to analyze the barrier energies. Dissection of the barrier energies established the basis set employed for each of the four molecular species by imposing the virial theorem criterion: $\Delta E + \Delta T \leq 100\ cm^{-1}$ (ΔE is the calculated barrier energy for the internal rotation process). This led to Hartree−Fock (HF) symmetry decomposition of barrier energies with basis sets ranging from 6-31G(2d,p) to 6-31++G(d,p) (individual molecule basis sets are listed in Tables 1 and 7). These calculations were carried out using GAUSSIAN 94 software[11] on the HP-UX 9000/735 CPU at the Rutgers Chemistry Department High Performance Computation Facility.

The relaxation calculations involved very tight geometry optimizations, carried out at both Hartree−Fock (HF) and second order Moller−Plesset (MP2) levels using the basis sets established for the energy partitioning calculations. Fully relaxed rotation allowed all coordinates to change from their optimized equilibrium values to top-of-barrier optimized ones; rigid rotation froze the geometry at the equilibrium one, except for the dihedral angle that describes methyl torsion; partially relaxed rotations froze certain coordinates at the equilibrium values and set others, as defined further in the text, at the fully relaxed values. The optimizations were carried out on the CRAY C90 processor at the Pittsburgh Supercomputer Center using GAUSSIAN 92 software.

Natural bond orbital (NBO)[12] calculations were carried out using NBO 4.0[13] interfaced to GAUSSIAN 94. Foster and Weinhold have shown the utility of natural atomic hybrid orbitals (NHO) in describing "orbital following" during ammonia umbrella inversion.[14] We utilize NBO 4.0 software to extract the NHOs for the five oxygen and sulfur lone-pair species under study. Steric interactions were calculated by the Badenhoop−Weinhold procedure using NBOs to obtain Pauli exchange repulsions.[15a] The NBO calculations were carried out on the processing equipment described under energy partitioning, except for some early steric calculations, which were carried out by Prof. Frank Weinhold on University of Wisconsin facilities at our request.

III. Oxygen-Containing Compounds

A. Barrier Energies. Partitioning of the barrier energy (the difference between the fully relaxed metastable state energy caused by 180° rotation of the methyl group(s) and the equilibrium state energy) into potential and kinetic energy terms (Table 1) shows that the only barrier-forming term is an increase in the nuclear−electron attraction energy, ΔV_{ne}, for the three oxygen-containing molecules. There are important quantitative differences, however: the ΔV_{ne} increase for dimethyl ether (DME) is much larger than for either protonated dimethyl ether or methanol. Further insight into barrier energetics is obtained by the dissection of ΔV_{ne} into symmetry components, given below.

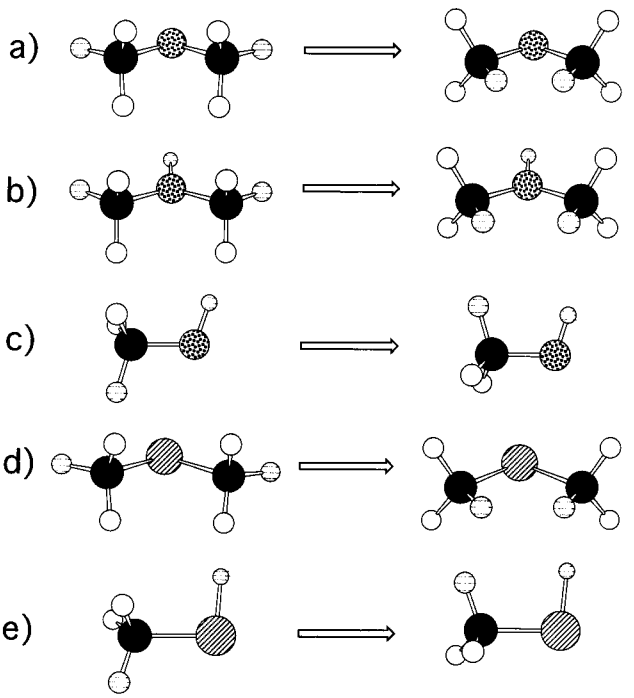

Figure 2. Equilibrium and top-of-barrier conformers: (a) dimethyl ether (DME), (b) protonated dimethyl ether (PDME), (c) methanol, (d) dimethyl sulfide (DMS), (e) methanethiol (MT). In-plane hydrogens are denoted by horizontal lines.

TABLE 2: Symmetry Dissection of the Nuclear−Electron Attraction Energy Change, ΔV_{ne}, Accompanying Fully Relaxed Internal Rotation in Oxygen-Containing Compounds (cm^{-1})[a]

ΔV_{ne}[b]	dimethyl ether (DME)	protonated dimethyl ether (PDME)	methanol
$A_1(\sigma)$	103 610	48 450	
$A_2(\pi)$	81 740	62 330	
$B_1(\pi)$	30 630	31 120	
$B_2(\sigma)$	22 000	−2920	
$A'(\sigma)$			28 560
$A''(\pi)$			−6480

[a,b] See footnotes *a* and *b* to Table 1.

1. Dimethyl Ether. DME illustrates the power of symmetry dissection. The equilibrium conformation C_{2v} symmetry is retained on going to the fully relaxed top of the barrier (Figure 2a), allowing ΔV_{ne} to be broken down into contributions from $a_1(\sigma)$, $a_2(\pi)$, $b_1(\pi)$, and $b_2(\sigma)$ orbitals (Table 2). The symmetry partitioning naturally separates π and σ effects and provides considerable surgical precision, since only the A_1 term contains the oxygen σ lone-pair reorganization energy. All symmetry classes are found to be barrier forming, with the largest barrier contribution originating from the $A_1(\sigma)$ term.[1] The broken "aromatic" stabilization model involving π bonding between the methyl groups and the oxygen atom in the equilibrium EE conformer[5] falls into the B_1 category. The next largest term involves doubly nodal a_2 orbitals requiring an increase in π antibonding character between the two methyl groups in the metastable top-of-the-barrier state. This increase must arise from π hyperconjugation since the oxygen nonbonding π orbital

TABLE 3: Optimized Geometries of Equilibrium and Top-of-Barrier Conformers[a]

	dimethyl ether HF/6-31G(2d,p)		methanol HF/6-31++G(d,p)		protonated dimethyl ether HF/6-311++G		dimethyl sulfide MP2 6-31G(2d,p)		methanethiol MP2 6-31++G(d,p)	
	EE	SS	E	S	EE	SS	EE	SS	E	S
bond lengths (Å)[b]										
C−X	1.3903	1.3945	1.4014	1.4049	1.4970	1.5020	1.8169	1.8305	1.8126	1.8212
C−H_{ip}	1.0823	1.0860	1.0812	1.0858	1.0736	1.0723	1.0881	1.0873	1.0908	1.0894
C−H_{op}	1.0896	1.0861	1.0872	1.0843	1.0733	1.0732	1.0889	1.0872	1.0902	1.0899
X−H			0.9423	0.9405	0.9489	0.9501			1.3342	1.3318
bond angles (deg)[b]										
C_a-X−C_b	113.7	118.6			122.7	126.2	98.0	102.3		
H_{ip}−C−X	107.7	112.2	107.1	112.0	106.1	105.7	107.4	109.8	106.6	110.5
H_{op}−C−X	111.5	109.8	111.8	109.5	106.6	106.8	110.7	109.8	111.7	110.0
H_{ip}−C−H_{op}	108.8	108.3	108.6	108.5	111.9	111.9	109.0	108.9		
H_{op}−C−H_{op}	108.4	108.5	109.0	108.8	113.1	113.2	109.9	109.5		
C−X-H			110.5	111.2	118.6	116.9			96.2	96.5

[a] Very tight optimization. [b] X designates oxygen or sulfur.

belongs to the b_1 representation, not a_2. The $B_2(\sigma)$ term, nearly as important as $B_1(\pi)$, can arise either from C−O bond orbitals or σ hyperconjugation interactions. It is noteworthy that the $A_1(\sigma)$ energy change overwhelms the barrier-forming contributions arising from the $b_1(\pi)$ orbitals. This conclusion does not preclude the possibility of a particular term in the B_1 symmetry class from being the single dominant barrier-forming term, but it is strongly suggestive. Further discussion is reserved for section D.

2. Protonated Dimethyl Ether. The idea that the barrier height in dimethyl ether mainly arises from oxygen σ lone-pair reorganization allows a clear prediction: *Structural or bonding changes that restrict lone-pair reorganization should lower the barrier*. Protonated dimethyl ether (PDME) allows this prediction to be put to a test, since the lone-pair in this species is tied up in the oxygen−proton bond. Although no experimental data are available, the test can be carried out by a computer experiment.

Figure 2 and Table 3 compare the predicted equilibrium and top-of-barrier geometries of DME and PDME. Both molecules possess C_{2v} symmetry. This symmetry is retained on rotation (Figure 2a,b); both molecules undergo COC angle opening (5° for DME and 3.5° for PDME). However, there are two important differences in the equilibrium geometries of DME and PDME that have a major impact on the internal rotation barrier: the COC angle 114° in DME has increased to 123° in PDME and the C−O bond length is predicted to be a full 0.1 Å longer in PDME.

The natural hybrid oxygen orbital compositions allow the changes in the DME oxygen σ lone-pair and the PDME bond-hybrid caused by internal rotation to be compared. As simple valence theory suggests,[16] the lone-pair rehydbridization in DME is much greater than for the oxygen bond-hybrid in PDME, the calculated p character increasing by nearly 3% (from 59.7% in the equilibrium conformation) in DME, but only by 1% (from 72.1%) in PDME.

The calculated PDME barrier (HF 6-311++G) is given in Table 1. The strong decrease from the 1600 cm^{-1} one in DME to only 300 cm^{-1} in PDME supports the important role of the oxygen atom electronic structure as a determinant for the barrier. The energy partitioning in Table 1 shows that ΔV_{ne}, the only barrier-forming term, is much smaller than in DME. Symmetry breakdown of ΔV_{ne} (Table 2) shows that this difference is mostly due to a strong decrease in the magnitude of the σ terms in PDME. The main reason for this decrease is the much reduced $A_1(\sigma)$ term. In DME σ terms dominate, and thus σ reorganization is the key change in this molecule during the rotation. In PDME, however, the π component dominates so that π interaction effects control the barrier. Moreover, the important B_1 π-ring-bonding term is virtually unchanged in the two molecules contrasted to the reduction of the leading A_1 symmetry σ term in DME on going to PDME. In summary, protonating the oxygen in DME leads to large barrier reduction and a reversal of the importance of σ and π orbitals in determining the barrier energy.

3. Methanol. Figure 2c shows the predicted HF 6-31++G(d,p) equilibrium (E) geometry of methanol. The C_s symmetry is retained on rotation to the top-of-the-barrier (S, Figure 2c); thus σ and π interaction changes fall into a′ and a″ symmetry categories, respectively. There is little change in bond lengths or in the COH angle, but in contrast to DME the methyl $H_{ip}CO$ angle increases by 5° (Table 3).

The HF 6-31++G(d,p) calculated methanol barrier is 400 cm^{-1} (Table 1), four times smaller than DME.[17] In the "aromatic" stabilization model, π-ring breaking accompanying internal rotation leads to an explanation of the reduction of the high DME barrier to a much smaller one in methanol. The Cremer−Binkley−Pople−Hehre picture of π interactions involving a cyclic structure of six bonding electrons,[5] proposed in 1974 for DME, was a precursor of the π fragment model[6] that is the accepted explanation for conjugated molecule methyl rotation barriers.

The central idea in the lone-pair rehybridization model that we are proposing is since there is little steric contact to open up the COH angle during methyl rotation, little change occurs in the methanol oxygen lone-pair during torsion. As shown in Figure 3, the increase in natural hybrid orbital p character accompanying internal rotation is only 1%, strongly reduced from the 3% increase in DME. In terms of the thinking we are presenting in this article, the much smaller oxygen σ lone-pair reorganization energy leads to a lower barrier.

The symmetry breakdown of ΔV_{ne}, given in Table 2, shows that $V_{ne}(\sigma)$ is greatly reduced and $V_{ne}(\pi)$ actually becomes <0, i.e., antibarrier. Consequently, only the σ term is barrier forming, and thus σ reorganization appears to be the key barrier energy determinant in methanol, unlike in PDME, where it is the π interactions that dominate. However, the lower symmetry present in methanol prevents the more detailed symmetry dissection possible for the bimethyl molecules.

B. Relaxation Effects. As shown in Table 3, the principal relaxations in DME are nearly 5° openings in both the COC and $H_{ip}CO$ angles. This latter angle opening is the only important relaxation in methanol. In PMDE a somewhat reduced (3.5°) COC angle opening is the only major relaxation. The effect of these relaxations on the barrier height is shown in Table 4 by comparing partially relaxed barrier energetics with the rigid rotation and fully relaxed ones given in Tables 4 and 2, respectively.

In each case the rigid rotation barrier is increased from the fully relaxed one: by 900 cm^{-1} for DME,[3] 280 for

TABLE 4: Relaxation Effects on the Symmetry Dissected Nuclear−Electron Attraction Energy Change, ΔV_{ne}, Accompanying Internal Rotation in Oxygen-Containing Compounds (cm^{-1})[a]

	relaxation[b]								
	dimethyl ether				protonated dimethyl ether		methanol		
ΔV_{ne}	rigid[d] rotation	COC angle	$H_{ip}CO$ angle	$H_{ip}CO$ & COC angles	rigid rotation	COC angle	rigid rotation	COH angle	$H_{ip}CO$ angle
barrier[c]	2480	2040	2060	1750	370	270	680	690	540
$A_1(\sigma)$	−46 070	31 780	6530	82 980	−16 450	13 990			
$A_2(\pi)$	74 610	88 910	75 900	90 110	49 490	57 910			
$B_1(\pi)$	18 560	41 340	20 140	42 430	10 410	18 610			
$B_2(\sigma)$	−128 810	−42 440	−76 430	6050	-68 770	−25 310			
$A'(\sigma)$							−10 300	−7630	22 220
$A''(\pi)$							5490	6350	3780

[a] Rounded to nearest 10 cm^{-1}. [b] All coordinates frozen at equilibrium conformation value except for the designated relaxation coordinate (which is relaxed to its value in the fully relaxed top-of-barrier conformation) plus rotation of the in-plane methyl hydrogen(s) by 180°. [c] Barrier calculated with the listed relaxations. [d] All coordinates frozen at equilibrium conformation except for rotation of in-plane methyl hydrogen(s) by 180°.

methanol, and 110 for PDME. Thus freezing relaxations lead to important increases of the fully relaxed barrier, ranging from 30% for PDME, 60% for DME, to 70% for methanol. Individual rigid rotation energy terms are even more dramatically changed from the fully relaxed ones. The electron−electron repulsion, ΔV_{ee}, increases, and ΔV_{ne} decreases for the three molecules. These senses are reversed from that for the fully relaxed process. Changes in the ΔV_{ne} symmetry decomposition are still more striking. In particular, the large barrier-forming totally symmetric σ energy term, dominant for fully relaxed internal rotation, becomes antibarrier, leaving only π terms barrier forming. Thus *for rigid rotation*, the barrier in all three oxygen-containing molecules appears to result from π electron interactions.

The effect of the COC angular opening in DME is to substantially lower the barrier (by nearly 500 cm^{-1}) from the rigid rotation one. The effect on the individual rigid rotation energetics is to alter them to ones qualitatively resembling the energetics found for fully relaxed rotation. The only disparity is in the $B_2(\sigma)$ term, which despite a large increase still remains antibarrier. The effect of angle openings is shown in considerable detail in Table 4. In contrast to the strong effect of COC angle opening on the σ energy terms, it has little effect on the π terms. The effect of $H_{ip}CO$ angle opening, although qualitatively in the same sense found for COC opening, is much smaller. By combining both angle openings the complete set of fully relaxed energetics, including the B_2 term and the barrier, itself, are semiquantitatively reproduced.

In PDME the 3.5° opening of the COC angle changes the sign of the $A_1(\sigma)$ term to barrier forming, while essentially leaving the π terms unaffected. However, the magnitude of the A_1 term is smaller than either of the π terms and much smaller than in DME. Thus COC angle opening, though even smaller in PDME than in DME, appears to play a key role in controlling the sign and magnitude of the $A_1(\sigma)$ ΔV_{ne} term, and consequently the barrier height.

The effect of $H_{ip}CO$ angle opening, the major relaxation in methanol, on ΔV_{ne} energetics is to change the sense of the $A'(\sigma)$ term to the barrier-forming one found for fully relaxed rotation. In contrast, the effect of the angle-opening relaxation on the relatively small $A''(\pi)$ term is weak. The effect of other flexings, e.g., COH angle opening and CO bond lengthening, is even weaker.

In summary, angle opening plays a key barrier energy role for all three oxygen-containing molecules. As might be expected, the effect of these angular distortions primarily involves the σ electrons.

C. Pauli Exchange Steric Repulsions. Table 5 summarizes *the changes* in Pauli exchange repulsions accompanying internal rotation, calculated for the three oxygen-containing molecules by the Badenhoop−Weinhold procedure.[15a] Badenhoop and Weinhold have shown that excellent agreement is obtained with the full ab initio potential curves for a number of rare gas and molecular steric contacts by these pairwise-additive interactions formulated in terms of NBOs.[15b]

TABLE 5: Principal Pauli Exchange Repulsion Changes Accompanying Internal Rotation (cm^{-1})[a]

	relaxation	C_a-H_{ip}/C_b-H_{ip}	$C-H_{ip}/X-H$[b,c]	$C-H_{ip}/lp(\sigma)X$[b,c]
DME	rigid rotation	4800		1400
	COC angle	2900		1600
	$H_{ip}CO$ angle	3500		1300
	fully relaxed	2000		1400
PDME	rigid rotation	600	500	
	COC angle	400	600	
	CO bond[d]	800	900	
	COC angle[d]	1300	800	
	COC angle & CO bond[d]	2400	1100	
	fully relaxed	400	600	
methanol	rigid rotation		500	1300
	COH angle		400	1300
	fully relaxed			1200
DMS	rigid rotation	2000		300
	CSC angle	1200		400
	CS bond	1900		200
	fully relaxed	900		300
MT	rigid rotation			500
	CSH angle			500
	fully relaxed			500

[a] Cutoff 0.5 kcal/mol (175 cm^{-1}), rounded to nearest 100 cm^{-1}. [b] See footnote *b*, Table 3. [c] There are two such repulsions in DME, PDME, and DMS. [d] For these relaxations the designated equilibrium coordinates are DME (EE) optimized values. The *changes* in these coordinates are for *PDME rotation*.

We start with fully relaxed rotation. As might be expected, the largest repulsion change is found between the two $C-H_{ip}$ bonds involving the two methyl groups in DME. The largest overlap is between these bonds ($|S(ij)| = 0.23$ for the EE conformer); consequently this pairwise interaction is found to give both the largest steric exchange energy and the largest differential exchange energy terms for internal rotation. This is greatly reduced (only one-fifth that of DME) in PDME. Another important term in DME, but not present in PDME, involves repulsion between the $O(\sigma)$ lone-pair and $C-H_{ip}$ bond. This latter interaction is the largest repulsion change in methanol with essentially the same magnitude as in DME. However, more significant to our understanding of the strains that cause the relaxations accompanying internal rotation (discussed in the preceding section) are the repulsion changes for rigid rotation. For DME rigid rotation the C_a-H_{ip}/C_b-H_{ip} repulsion change is nearly 5000 cm^{-1}, more than double that for fully relaxed

rotation. In contrast, the much smaller PDME repulsion change involving the same bonds is little altered. In methanol, the dominant lp(σ)O/C−H_{ip} repulsion change term is also essentially invariant to whether the rotation is fully relaxed or rigid.

A still more insightful understanding of these strains is given by the repulsion changes for the important (individual) skeletal flexings discussed in section B. These partially relaxed rotations, defined by freezing all flexing coordinates at their equilibrium values except one, allow the impact of relaxation of a single coordinate to be investigated.

The effect of the partial relaxation involving COC angle opening alone on the large C_a−H_{ip}/C_b−H_{ip} repulsion change occurring for rigid rotation in DME is the salient feature of our discussion: *the repulsion decreases to nearly that for fully relaxed rotation*. But there is little effect on the remaining important repulsion, between the O(σ) lone-pair and the C−H_{ip} bond, lp(σ)O/C−H_{ip}. Other partial relaxation effects are not as dramatic; the only other important example is H_{ip}CO angle opening (Table 5).

That the low repulsion between the two C−H_{ip} bonds in PDME is due to both the increased equilibrium conformer COC angle and the longer C−O bond length compared to DME is shown by three artificial flexing calculations (shown in italics in Table 5). The first sets the equilibrium conformer bond angle equal to the COC angle in DME (114°). The second sets the equilibrium bond length equal to the C−O bond length in DME (1.390 Å). The final calculation incorporates both constraints. The *changes* in these parameters on going to the top of the barrier are taken as the changes calculated for fully relaxed PDME internal rotation. All other geometrical parameters are the appropriate PDME fully relaxed ones. As shown in Table 5, the increase in the C_a−H_{ip}/C_b−H_{ip} repulsion term is more pronounced when the DME angle is adopted. But, the increase only approximates that for DME when both DME COC angle and C−O bond length values are assumed for the PDME equilibrium conformer.

D. Natural Bond Orbital Analysis. Natural bond orbital (NBO) analysis transforms molecular orbital wave functions into one-center (lone-pair) and two-center (bond) representations.[12] Weinhold has shown how this kind of categorization represents a chemically appealing point of view, since it throws a spotlight on the individual bonds and lone-pairs that play a role in a chemical process.[18] The diagonal elements of the Fock matrix in an NBO representation represent the energies of localized bonds, antibonds, and lone-pairs. Off-diagonal elements represent bond−antibond, lone-pair−antibond, and normally neglectably small antibond−antibond interactions.

We now use this scheme to dissect the barrier energy into bond and lone-pair energies. This decomposition, when combined with the symmetry and flexing analyses given in sections B and C, leads to a transparent understanding of the barrier energy. Bond−antibond and lone-pair−antibond interactions are also considered for their complementary roles to steric effects in influencing the flexing relaxations that accompany internal rotation.

Table 6 shows the principal bond and lone-pair energy changes, $\Delta\omega$, accompanying internal rotation for the three oxygen-containing molecules. These have been obtained from the relation

$$\Delta\omega = \epsilon_t N_t - \epsilon_e N_e \qquad (1)$$

where ϵ_t and ϵ_e represent NBO energies for the top-of-barrier and equilibrium conformers, respectively, and N_t and N_e are the corresponding NBO occupancies. Since we are primarily interested in the most important determinants of the barrier energy, only the principle interactions are included in Table 6,

TABLE 6: Principal Barrier-Forming Bond and Lone-Pair Energy Terms for the Oxygen-Containing Compounds (cm^{-1})[a]

	barrier contribution[c]		
NBO[b]	dimethyl ether	protonated dimethyl ether	methanol
lp(σ)O	12 300		3200
O−H^+		5400	
C−H_{op}	1700[d]	300[d]	2300[e]
O−C(σ)		800[e]	1500
lp(π)O		200	400

[a] Fully relaxed internal rotation. Values are rounded to nearest 100 cm^{-1}. [b] Natural bond orbital. [c] Where there are multiple identical orbitals, the contribution of only one is given. [d] There are four such orbitals. [e] There are two such orbitals.

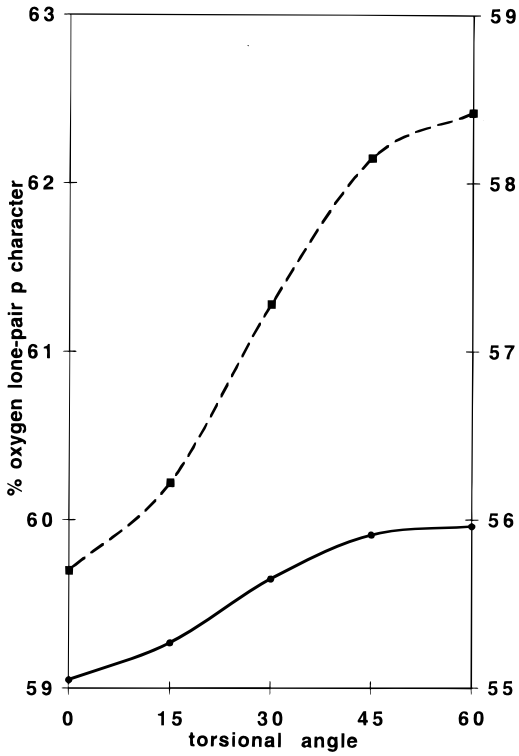

Figure 3. Dependence of oxygen lone-pair p character on methyl torsional angle. Dashed curve: dimethyl ether. Solid curve: methanol. Left-hand scale: DME. Right-hand scale: methanol.

with magnitudes rounded off to the nearest 100 cm^{-1}. For DME, the one term giving by far the most important barrier contribution involves the oxygen lone-pair, lp(σ)O. Since this term can only involve an a_1 orbital, the origin of the large A_1 barrier-forming energy discussed in section B is the reorganization of lp(σ)O displayed in Figure 1. The only other significant barrier contribution involves weakening of the C−H_{op} bond, whose bonding type (σ or π) cannot be unambiguously specified. The lone-pair reorganization term virtually vanishes in PDME; it is replaced by the much smaller O−H^+ term involving weakening of the O−H^+ bond, explaining the large reduction found for the A_1 barrier-forming energy in PDME. The oxygen σ lone-pair still exists in methanol; however its contribution to the barrier is reduced to only one-quarter that in DME (Table 6). The small gain in p character (Figure 3) explains why its barrier energy role is sharply reduced. Lack of sterically driven COH angular distortion in methanol rationalizes the small p character increase. In methanol the lp(σ)O reorganization is so reduced that C−H_{op} bond weakening is greater in importance.

Calculation of bond−antibond interaction energies is not as straightforward as the bond and lone-pair energies. They were estimated by two procedures. The first involves an indirect

TABLE 7: Principal Barrier-Forming Bond−Antibond Interaction Terms in the Oxygen-Containing Compounds (cm^{-1})[a]

	barrier contribution[b]		
donor/acceptor	dimethyl ether	protonated dimethyl ether	methanol
C_a-H_{ip}/O−C_b* [c]	1500	1000	
C−H_{ip}/O−H*			1100
O−C_b/C_a-H_{ip}* [c]	600		
O−H/C−H_{ip}*			500
C−H_{op}/O−H* [d]		300	
lp(π)O/C−H_{op}*	500[d]		200[c]
lp(σ)O/C−H_{op}*	600[d]		200[c]

[a] See footnote *a*, Table 6. [b] Where there are multiple identical interactions, the contribution of only one is given. [c] There are two such interactions. [d] There are four such interactions, two for each carbon.

procedure discussed in detail by Weinhold,[19] which involves comparison of barrier energies calculated with and without the Fock matrix element, F_{ij*}, between bonding (or lone-pair) NBO (occupancy near 2) and a virtually unoccupied antibonding orbital, deleted, the second by second-order perturbation theory $F_{ij*}^2/(\epsilon_i - \epsilon_j)$. The principal bond−antibond interaction energies estimated by the latter procedure are given in Table 7. In all cases the two procedures give semiquantitatively similar interaction energies.

Part of the importance of these interactions lies in their associated bond−antibond charge transfers. The most important barrier-forming interactions involve C_a−H_{ip} and O−C_b (DME and PDME) or O−H (methanol) bonds and antibonds. The only significant contribution to the DME and PDME barrier energies is the interaction C_a−H_{ip}/O−C_b*, involving charge transfer from one of the C−H_{ip} σ bonds to the O−C* (σ) antibond. However, while not negligible, this interaction provides for either molecule a much less important barrier energy contribution than the largest bond/lone-pair energy contributions shown in Table 6. The C−H_{ip}/O−H* barrier-forming interaction in methanol (involving charge transfer from one of the C−H_{ip} bonds to the O−H* σ antibond) is also much smaller than the lone-pair barrier energy contribution, but its relative importance is greater than any of the bond−antibond interactions for any of the molecules studied. Figure 4a depicts the orbitals involved in this interaction for the eclipsed conformation, showing the significant favorable overlap (evidenced by the Fock matrix element, $F_{ij*} = 39$ kcal/mol). In contrast, the same orbitals plotted in Figure 4b with the C_{me}−H_{ip} bond in the staggered geometry show markedly decreased overlap (reducing F_{ij*} to 6 kcal/mol), explaining why this interaction, involving charge transfer from the methyl group into the O−H region, is a significant barrier-forming interaction in methanol.

There is an antibarrier interaction in methanol with special importance. This is the C−H_{op}/O−H* interaction with magnitude $=400$ cm^{-1} (there are two such terms). Its importance is that it is the only antibarrier term that can involve π electrons. *It allows rationalization of both the antibarrier A″(π) ΔV_{ne} and methyl C−H_{op} bond weakening terms found for this molecule (Tables 2 and 6) in terms of charge transfer of bonding C−H_{op} density into a O−H antibonding orbital.*

IV. Sulfur-Containing Compounds

We now extend this idea of the significance of lone-pair σ orbital reorganization in controlling methyl internal rotation barriers in oxygen-containing molecules to the sulfur analogs of DME and methanol. The in-depth understanding obtained for the sulfur compound barriers illustrates both the utility of the electronic reorganization effects that we are discussing and

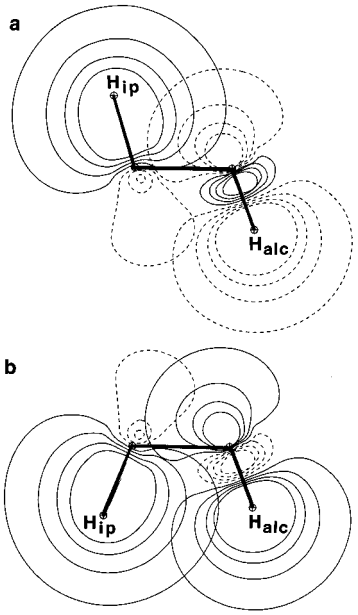

Figure 4. Orbital contour diagrams for methanol C−H_{ip} bonding and O−H_{alc}* antibonding pre-NBO (not orthogonalized) in (a) equilibrium and (b) top-of-barrier (staggered) conformations illustrating the more favorable overlap for the equilibrium conformation. The in-skeletal-plane contours increase by 0.01 with each contour (the outermost contour is at 0.04).

TABLE 8: Symmetry Dissection of the Nuclear−Electron Attraction Energy Change, ΔV_{ne}, Accompanying Fully Relaxed Internal Rotation in Sulfur-Containing Compounds (cm^{-1})[a]

	dimethyl sulfide (DMS) EE→SS	methanethiol (MT) E→S
ΔV_{ne}[b]	HF/6-31G(2d,p)	HF/6-31++G(d,p)
barrier	1480	480
$A_1(\sigma)$	164 550	
$A_2(\pi)$	81 990	
$B_1(\pi)$	67 670	
$B_2(\sigma)$	63 910	
A′(σ)		57 300
A″(π)		13 150

[a,b] See footnotes *a* and *b*, Table 1.

the power of *combined* NBO relaxation analysis to provide an in-depth understanding of barriers in floppy molecules, in general.

A. Dimethyl Sulfide. The C_{2v} symmetry equilibrium EE predicted structure (MP2 6-31G(2d,p)) is similar to DME (Figure 2d). As in DME, this symmetry is retained on going to the SS top-of-barrier conformation. There are important differences, however. As expected from simple valence considerations, the C−S bond is longer than the C−O one and the CSC angle in the equilibrium conformer is smaller (Table 3) than the COC angle. Another important difference is the increase in C−S bond length by >0.01 Å in the SS conformer, much larger than the C−O lengthening in DME. These differences, overall, are expected to lead to much reduced steric contact in DMS from that in DME. The result is reduced CSC angle opening in DMS (3.5°) from the 5° COC angle opening that accompanies methyl group rotation in DME. In accord with structural rules, smaller lone-pair reorganization effects are expected,[20] with a consequent much lowered barrier. As shown in Table 8 *the calculated DMS barrier*[21] *is close to that in DME, contrary to this prediction.*

There are parallels between the energy partitionings found for DME and DMS: for fully relaxed internal rotation only nuclear−electron attraction is barrier forming. As in DME all symmetry classes are barrier forming, with the largest contribu-

TABLE 9: Principal Barrier-Forming Bond and Lone-Pair Energy Terms for the Sulfur-Containing Compounds (cm^{-1})[a]

	barrier contribution[c]	
NBO[b]	dimethyl sulfide	methanethiol
lp(σ)S	4500	900
C−H_{op}	700[d]	900[e]
S−C(σ)	3300[e]	2700

[a] Fully relaxed internal rotation. Also see footnote *a*, Table 4. [b−e] See corresponding footnotes, Table 6.

tion originating from the $A_1(\sigma)$ term. Furthermore, the ordering ΔV_{ne} $A_1(\sigma) > A_2(\pi) > B_1(\pi) > B_2(\sigma)$ is the same. In essence symmetry partitioning rationalizes the large barrier calculated for DMS, but it does not explain why.

Little clue is provided by relaxed rotation energetics since these are remarkably similar for both molecules (compare Tables 2 and 8). As foreseen by the the longer C−S bond length in DMS, the principal Pauli exchange steric repulsion changes are strongly reduced (for both rigid and fully relaxed rotations) in DMS from their values in DME (Table 5). Expansion of the CSC angle to its value in the SS conformer greatly lowers the dominant C_a-H_{ip}/C_b-H_{ip} repulsion, but C−S bond lengthening has little effect (Table 5), indicating that the 3.5° angle opening is driven by steric contact between the in-plane C−H bonds. However, it requires *combined* methyl group and CSC angle relaxations to reduce this repulsion to the fully relaxed value.

The smoking gun that explains the high barrier is provided by the NBO analysis given in Table 9. In contrast to the single large lp(σ)O term in DME, there are two major barrier-forming terms in DMS: lp(σ)S and S−C(σ). While σ lone-pair reorganization persists in DMS, its contribution to the barrier is only one-third that of DME, in accord with the small gain in p character.[20] Thus the lone-pair reorganization term in DMS is strongly reduced from its oxygen counterpart, as predicted. But the S−C(σ) term, involving weakening of the S−C(σ) bond, compensates for the reduced lone-pair reorganization energy. Since there are two sulfur−carbon bonds, their weakening gives the most important barrier contribution and rationalizes the large A_1 barrier-forming energy.

In contrast to DME, large barrier-forming bond−antibond interactions are absent, probably because of reduced overlap with sulfur third-shell orbitals. In particular the analog of the important $C_a-H_{ip}/O-C_b$* term in DME (Table 7) is reduced to only 500 cm^{-1} in DMS. The origin of C−S bond weakening is more subtle; one possibility is that it is due to bending of the C−S bond. The calculated deviation of the C−S bond sulfur σ-NHO from the bond axis is 1.9° in the equilibrium conformation, but increases to 3.5° in the SS one (Figure 5c,d). The weakening then would stem from vulnerability of the relatively weak C−S bond (∼170 kcal/mol compared to ∼260 kcal/mol for C−O) to the charge displacement (compare to the *decrease* in deviation for the C−O bond NHO in the rotated DME conformer (Figure 5a,b)).[22]

B. Methanethiol. The predicted MP2 6-31++G(2d,p) equilibrium (E) geometry of methanethiol (MT) is given in Table 3. The C_s symmetry is retained on rotation to the S top-of-barrier metastable conformer. In these respects MT is similar to methanol; however the C−S and S−H bond lengths, as expected, are much greater than the equivalent bonds in methanol. Comparison of the CSH and COH equilibrium conformer angles reveals another important difference: the thiol one, at 98°, is much smaller than the 111° alcohol angle. The major angular relaxation accompanying methyl torsion is similar in the two molecules: expansion of the methyl $H_{ip}CO$ and $H_{ip}CS$ angles. However, the C−S bond lengthens by 0.009 Å in MT contrasted to only 0.0035 Å C−O lengthening in methanol. On

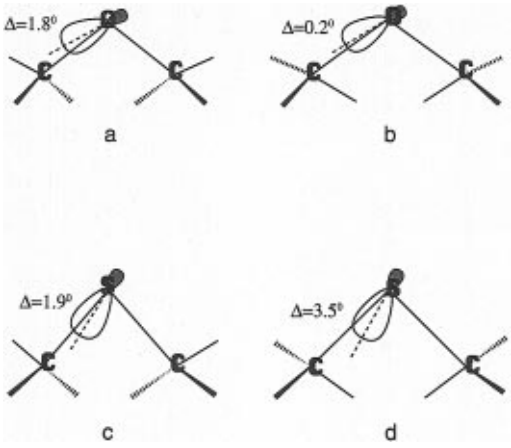

Figure 5. Calculated deviations (△) of oxygen (top) and sulfur (bottom) natural hybrid bond orbitals from C−X bond lines in dimethyl ether and dimethyl sulfide in the equilibrium (a and c) and SS (b and d) conformers illustrating the increased deviation in the top-of-barrier conformer for DMS. The drawn deviations have been exaggerated for clarity.

the basis of the importance of S−C(σ) bond weakening in controlling the DMS barrier height, S−C bond weakening is predicted to be an important barrier determinant in MT. Its overall role, however, is expected to be smaller than in DMS because of the single sulfur−carbon bond in MT. Since S−C bond weakening compensates for the reduced lone-pair reorganization energy on the sulfur atom (compared to oxygen), the MT barrier is not expected to be very different from methanol. This expectation is born out by the HF 6-31++G(2d,p) 480 cm^{-1} calculated barrier,[23] somewhat higher than the 400 cm^{-1} one in methanol.

Dissection of the MT barrier shows that the increase in V_{ne} accompanying fully relaxed internal rotation is much smaller than for DMS, parallel to the difference found between DME and methanol. However, symmetry decomposition (Table 8) shows an important difference between MT and methanol: while the σ term remains strongly dominant (as in methanol), $\Delta V_{ne}(\pi)$ is barrier forming, unlike the antibarrier π term in methanol.

The NBO analysis given in Table 9 allows several conclusions. The major barrier forming term in MT is weakening of the S−C(σ) bond, compensating for the reduction of the lone-pair reorganization term, lp(σ)S, from the lp(σ)O term in methanol, as expected. There is also a much reduced importance of methyl C−H_{op} bond weakening compared to methanol. As is the case for DMS, bond−antibond interactions are small in MT. In particular, the lp O/C−H_{op}* interactions, significant in methanol, are small (i.e. <0.5 kcal/mol) in MT, pointing to lowered importance of hyperconjugative interactions (because of less favorable sulfur 3p-methyl-hyperconjugative overlap) as the source of the reduced C−H_{op} bond weakening in MT.

V. Conclusions

The unified approach to barrier energetics, combining natural bond orbital, symmetry, and relaxation analyses given in the preceding sections, demonstrates that oxygen lone-pairs play an important (sometimes dominant) role in controlling barrier heights. An in-depth understanding of barrier formation and energetics for dimethyl ether, protonated dimethyl ether, and methanol is provided by dissecting the barrier into three key sources: Pauli exchange steric repulsion, oxygen σ lone-pair reorganization, and π hyperconjugation.

In DME the increased steric contact brought about by simultaneous internal rotation of the methyl groups causes the COC angle to increase, in turn increasing electron-pair repulsion between the oxygen σ lone-pair and C−O bonding pairs. The

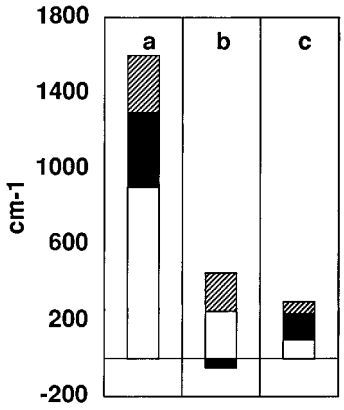

Figure 6. Schematic depiction of oxygen compound internal rotation barrier energetics. Open: σ reorganization. Solid: π interaction. Diagonal: steric exchange repulsion. (a) DME, (b) methanol, (c) PDME.

increased electron-pair repulsion is minimized by increased lone-pair p character, causing it to move further away from the oxygen atom.[24] *It is the lone-pair reorganization energy that controls the DME barrier height.* Methyl hyperconjugation and steric repulsion play minor roles as far as the barrier energy is concerned (even though the steric contact can be looked at as the origin of the lone-pair increased p character). This picture of DME barrier energetics is illustrated in Figure 6a.[25]

This mechanism for the barrier origin in DME allows the effect of acidic media on the barrier height to be predicted and an appreciation of why the barrier is drastically lowered in methanol to be obtained. In both cases there is decreased steric contact involving the methyl group(s). The outcome is strongly reduced oxygen atom p character change. The resulting lowered lone-pair reorganization energy and absence of important barrier-forming π interactions explain the low barrier in methanol (Figure 6b). *In PDME it is the increased acidity of the SS conformer that is the principal determinant of the barrier height* (Figure 6c). σ lone-pair reorganization alone is too simple as a model for media effects,[26] but its key feature, oxygen atom focused reorganization, allows the clear prediction that *acid media effects on DME are to strongly reduce the barrier*.

Extension to the sulfur analogs of DME and methanol illustrates the usefulness of these ideas. Lone-pair σ reorganization effects decrease in sulfur compounds compared to the oxygen-containing ones. However, the longer C−S bond is more vulnerable to charge displacement effects (such as bond-bending) and thus is weakened in the metastable top-of-barrier state. The two antagonistic effects then leave the barrier little changed from the oxygen analogs. Another application is to hexafluorodimethyl ether. Compared to DME there is increased steric repulsion, but there is now the electron-withdrawing effect of the CF_3 groups on the oxygen lone-pair. The increased steric factor should increase the lone-pair reorganization energy compared to DME, but the electron-withdrawing factor should decrease it. A recent computational study of the internal rotation barrier in this molecule[27] concludes that the barrier to the half-rotated molecule (SE), where the steric effect is minimized, is greatly reduced from that in DME and slightly reduced for simultaneous CF_3 group rotation to the SS conformer.

There have been a number of recent attempts at rationalizing rotational barriers in terms of individual atom energy changes, e.g., atomic basins used by Bader, Cheeseman, and Wiberg[28] and atomic indices by Knight and Allen.[29] These attempts have suffered in general from a lack of easy identification with accepted chemical-bonding concepts and also from a lack of facile transferability of the atomic properties employed from one molecule to another. The springboard for our discussion of the role of lone-pair reorganization effects on barrier origins in oxygen- and sulfur-containing molecules is Foster and Weinhold's 1980 paper on natural hybrid orbitals.[14] We have shown the utility of these orbitals for the analysis of changes both within a single molecule and between related molecules. In this article we have focused our discussion of lone-pair reorganization effects on barrier heights; a subsequent publication will discuss their influence on barrier widths and shapes and consequently on internal rotation dynamics.

Acknowledgment. We thank Professor Frank Weinhold for many helpful discussions concerning NBO calculation procedures and for calculating some of the Pauli exchange repulsions. Support by the National Science Foundation and a C-90 time grant from the Pittsburgh Supercomputer Center are gratefully acknowledged.

References and Notes

(1) Goodman, L.; Pophristic, V. *Chem. Phys. Lett.* **1996**, *259*, 287.
(2) Senent, M. L.; Moule, D. C.; Smeyers, Y. G. *Can. J. Phys.* **1995**, *73*, 425.
(3) Ozkabak, A. G.; Goodman, L. *Chem. Phys. Lett.* **1991**, *176*, 19.
(4) Fontaine, M.; Delhalle, J.; Defranceshi, M.; Bourin, J. M. *J. Mol. Struct.* **1996**, *300*, 607.
(5) Cremer, D.; Binkley, J. S.; Pople J. A.; Hehre W. J. *J. Am. Chem. Soc.* **1974**, *96*, 6900.
(6) Hehre, W. J.; Pople, J. A.; Devaquet, A. J. P. *J. Am. Chem. Soc.* **1976**, *98*, 664.
(7) Sovers, O. J.; Kern, C. W.; Pitzer, R. M.; Karplus, M. *J. Chem. Phys.* **1968**, *49*, 2592.
(8) (a) Scharnagl, C.; Fischer, S. F. *Chem. Phys.* **1996**, *212*, 231. (b) Wesche, D. *Antimicrob. Agents Chemother.* **1994**, *38*, 1813. (c) Estiu, G. L. *J. Mol. Struct. (THEOCHEM)*, in press. (d) Capizzi, R. L. *Leuk. Lymphoma* **1993**, *10*, Suppl., 147.
(9) (a) Houk, K. N.; Williams, J. C., Jr.; Mitchell, P. A.; Yamaguchi, K. *J. Am. Chem. Soc.* **1981**, *103*, 949. (b) Broeker, J. L.; Hoffmann, R. W.; Houk, K. N. *J. Am. Chem. Soc.* **1991**, *113*, 5006. (c) Knochenmuss, R.; Muino, P. L.; Wickleder, C. *J. Phys. Chem* **1996**, *100*, 11218.
(10) Catalan, J.; de Paz, J. L. G.; del Valle, J. C.; Kasha, M. *J. Phys. Chem.*, in press.
(11) Frisch, M. J.; Trucks, G. H.; Schlegel, H. B.; Gill, P. M. W.; Johnson, B. J.; Robb, M. A.; Cheeseman, J. R.; Keith, T; Petersson, G. A.; Montgomery, J. A.; Raghavachari, K.; Al-Laham, M. A.; Zakrzewski, V. G.; Ortiz, J. V.; Foresman, J. B.; Cioslowski, J.; Stefanov, B. B.; Nanayakkara, A.; Challacombe, M.; Peng, C. Y.; Ayala, P. Y.; Chen, W.; Wong, M. W.; Andres, J. L.; Replogle, E. S.; Gomperts, R.; Martin, R. L.; Fox, D. J.; Binkley, J. S.; Defrees, D. J.; Baker, J.; Stewart, J. P.; Head-Gordon, M.; Gonzalz, C.; Pople, J. A. *GAUSSIAN 94*; Gaussian, Inc.: Pittsburgh, PA, 1995.
(12) Reed, A. E.; Weinhold, F. *J. Chem. Phys.* **1983**, *78*, 4066.
(13) Glendening, E. D.; Badenhoop, J. K.; Reed, A. E.; Carpenter, J. E.; Weinhold, F. *NBO 4.0*; Theoretical Chemistry Institute: University of Wisconsin, Madison, 1996.
(14) Foster, J. P.; Weinhold, F. *J. Am. Chem. Soc.* **1980**, *102*, 7211.
(15) (a) Badenhoop, J. K.; Weinhold, F. *J. Chem. Phys.*, in press. (b) Badenhoop, J. K.; Weinhold, F. *J. Chem. Phys.*, in press.
(16) Bent, H. A. *Chem. Rev.* **1961**, *61*, 899.
(17) Chung-Phillips, A.; Jebber, K. A. *J. Chem. Phys.* **1995**, *102*, 7080.
(18) Reed, A. E.; Curtiss, L. A.; Weinhold, F. *Chem. Rev.* **1988**, *88*, 899.
(19) Reed, A. E.; Weinhold, F. *Isr. J. Chem.* **1991**, *31*, 277.
(20) In DMS the lone-pair changes from $sp^{0.48}$ (% p = 32.3) in the equilibrium conformer to $sp^{0.49}$ (% p = 33.0) at the barrier top.
(21) (a) Pierce, L.; Hayashi, M. *J. Chem. Phys.* **1961**, *35*, 479. (b) Senent, M. L.; Moule, D. C.; Smeyers, Y. G. *J. Phys. Chem.* **1995**, *99*, 7970.
(22) The C−O bond is calculated to strengthen in the DME rotated conformer.
(23) Colson, A. O.; Sevilla, M. D. *J. Phys. Chem.* **1994**, *98*, 10484.
(24) The repulsions listed in Table 5 have already taken into account the lone-pair reorganization.
(25) The magnitudes in Figure 6a are slightly altered from Figure 3a in ref 1 because the more extended basis set reported here has been utilized.
(26) For example: Smith, M. J.; Krogh-Jespersen, K.; Levy, R. M. *Chem. Phys.* **1993**, *171*, 97.
(27) Bouno, R. A; Zauhar, R. J; Venanzi, C. A. *J. Mol. Struct. (THEOCHEM)* **1996**, *370*, 97.
(28) Bader, R. F. W.; Cheeseman, K. E.; Laidig, K. E.; Wiberg, K. B.; Breneman, C. J. *J. Am. Chem. Soc.* **1990**, *112*, 6530.
(29) Knight, E. T.; Allen, L. C. *J. Am. Chem. Soc.* **1995**, *117*, 4401.